

Local structures in zincblende-type random solid solutions

This article has been downloaded from IOPscience. Please scroll down to see the full text article.

1994 J. Phys.: Condens. Matter 6 4437

(<http://iopscience.iop.org/0953-8984/6/24/006>)

View [the table of contents for this issue](#), or go to the [journal homepage](#) for more

Download details:

IP Address: 171.66.16.147

The article was downloaded on 12/05/2010 at 18:37

Please note that [terms and conditions apply](#).

Local structures in zincblende-type random solid solutions

Wu Zhonghua and Lu Kunquan

Institute of Physics, Chinese Academy of Sciences, Beijing 100083, People's Republic of China

Received 25 January 1994

Abstract. The local structures of zincblende-type solid solutions $A_{1-x}B_xC$ can be described with five distorted unit cells based on a phenomenological valence force-field approach. Bond lengths and strain energies in these solid solutions can be obtained. The distorted feature of the local structure is well described by the five distorted unit cells. This structural model has been applied to 18 $A_{1-x}B_xC$ systems. Results are compared with those from extended x-ray absorption fine structure and demonstrate that all the first- and second-neighbour bond lengths are in agreement with experimental values, with the largest divergence being about 0.01 Å. In addition, this model is also compared with the five special tetrahedra model.

1. Introduction

Zincblende-type random solid solutions, formulated as $A_{1-x}B_xC$ or $AC_{1-x}D_x$, belong to $F43m$ space group. The only difference between $A_{1-x}B_xC$ and $AC_{1-x}D_x$ is that the former is anion-sharing and the latter is cation-sharing. For convenience, we do not distinguish $A_{1-x}B_xC$ from $AC_{1-x}D_x$, and we consider only the former. The cations A and B randomly occupy one set of face-centred cubic (FCC) positions, and the anions C occupy the other set. Previous x-ray diffraction confirmed that the lattice constants of almost all pseudobinary zincblende-type random solid solutions obey Vegard's law. Under the virtual crystal approximation (VCA) model, the first- and second-neighbour bond lengths are $\sqrt{3}a(x)/4$ and $\sqrt{2}a(x)/2$, respectively, where $a(x)$ is the lattice constant of the solid solutions at composition x . That is to say, the unit cells of the solid solutions are continuously expanded or contracted with composition. On the other hand, Pauling's notions suggest that bond lengths and bond angles are approximately conservative quantities in different chemical environments. Hence bond lengths and bond angles in solid solutions keep the same values as in the pure end compounds. In this case, solid solutions are equivalent to mixtures of two types of unit cells originating from the two pure end compounds. Recent extended x-ray absorption fine structure (EXAFS) experiments [1-6] show that the first-neighbour A-C and B-C bond lengths as well as the second-neighbour C-A-C and C-B-C bond lengths tend to retain the respective values in the pure end compounds, but the second-neighbour A-C-A, A-C-B and B-C-B bond lengths approach those expected from the VCA model. It can be seen that the VCA model and Pauling's notions are two limiting possibilities. In fact, there are some distortions in the local structures of zincblende-type random solid solutions. How to accommodate these distortions is worthy of study. Some theoretical calculations such as the quasichemical approximation (QCA) [7], *ab initio* pseudofunction total-energy calculation [8], valence force-field (VFF) approach [3, 9-19], Monte Carlo simulation [20] and so on, were employed to treat this problem. Among them, the VFF approach has been widely applied because of its conceptual simplicity and because the calculations are less

time-consuming. This phenomenological VFF theory is simple and convenient to predict the effects of strain on such structural features as bond lengths. Cai and Thorpe (CT) [17] derived an analytic solution for the quaternary zincblende alloys $A_{1-x}B_xC_{1-y}D_y$, based on the Kirkwood model [21]. The CT theory was further applied to pseudobinary zincblende alloys $A_{1-x}B_xC$ [18] and the binary alloy $Si_{1-x}Ge_x$ [19]. Previous work [11, 16, 18] implied that the geometrical configuration plays the dominant role in the bond lengths. In this paper, starting from the microscopic geometrical configuration, we propose a statistical model that involves five distorted unit cells (FDUC) with the binomial Bernoulli distribution. The Harrison model [11, 22] of VFF theory is used to determine the equilibrium bond lengths and the strain energies of the five distorted unit cells. The FDUC model is applied to 18 $A_{1-x}B_xC$ systems and predicts the distorted feature of the local structure and the relative strain energy. Both the first- and second-neighbour bond lengths are in excellent agreement with those from EXAFS.

2. Local structural model

EXAFS results are an average effect over possible local structures, and x-ray diffraction results reflect the average over EXAFS results. This implies that a model describing the local structures of solid solutions must be statistical, and the selected structure units must be independent of their environments so that their energy expression is also independent of the environments. In our previous work [5], the five special tetrahedra (FST) model was used to describe $GaAs_xP_{1-x}$ solid solutions. The first-neighbour bond lengths and the anion-anion second bond lengths can be excellently reconstructed, but information about the cation-cation second bond lengths cannot be obtained. It is thus clear that the FST model is not satisfactory. Let us check the unit cells of pseudobinary $A_{1-x}B_xC$ solid solutions again. The cations A and B distribute randomly in the cation sublattice, and the anions C occupy the anion sublattice. We select unit cells like that shown in figure 1. Evidently there are four cations A and/or B inside the unit cell. Only five different unit cells can be found with n B-type atoms and $4 - n$ A-type atoms ($n = 0, 1, 2, 3, 4$), respectively. The possibility of finding a unit cell with n B-type atoms and $4 - n$ A-type atoms can be described with the binomial Bernoulli distribution [3, 5]:

$$P(n, x) = \binom{4}{n} x^n (1-x)^{4-n} \quad (n = 0, 1, 2, 3, 4). \quad (1)$$

Here, x is the composition of $A_{1-x}B_xC$ solid solutions.

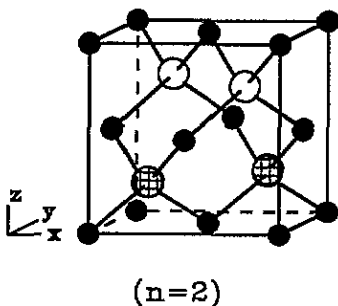


Figure 1. Distorted unit cell in $A_{1-x}B_xC$ solid solutions. It contains n B atoms and $4 - n$ A atoms ($n = 0, 1, 2, 3, 4$), respectively. Note that the unit cell shown with $n = 2$ is undistorted from the parent zincblende form. Cations A and B are shown as large open and hatched circles, respectively, and the anions C are shown as smaller filled circles.

Schabel and Martins [16] studied the convergence of elastic energy with supercell size. Their results demonstrated that the average energy per atom dropped from 1.26 to 1.18 mRyd when the supercell size was increased from eight to 64 atoms. Use of a larger cell with 216 atoms results in an insignificant increase in the energy of 0.02 mRyd/atom. This illustrates clearly that the near-neighbour interaction is dominant in diamond-like and zincblende-type crystals. So we assume that the influence of disorder beyond the unit cells does not affect the local distortion inside the unit cells, and the five distorted unit cells are independent of each other. The long-range effects are much smaller than the local ones even if it is not necessary to assume that they are negligible. The net influence acting on the unit cells will be close to zero. This allows us to deal with the strain energy independently for each distorted unit cell and to count the local structure parameters according to the binomial Bernoulli distribution. So only these interatomic actions inside each distorted unit cell need to be included. The five distorted unit cells are selected to be independent structural units.

Obviously because A and B atoms have different sizes, as well as A-C and B-C bonds have different bond strengths, the lattice sizes are different and the atoms do not locate at regular positions in the five unit cells. The unit cell with $n = 0$ (or $n = 4$) is completely the same as in pure AC (or BC) compounds with no distortion. The two unit cells with $n = 1$ and $n = 3$ have the same distorted features with a symmetrical axis along $\langle 111 \rangle$ direction. For the unit cell with $n = 2$, besides the distortions along z direction, there are also distortions in the middle xy plane. We assume that the shapes of the five distorted unit cells still remain cubic. X-ray diffraction demonstrates that almost all lattice parameters obey Vegard's law in zincblende-type solid solutions. For the three distorted unit cells with $n = 1, 2$ and 3 B-type atoms, it is natural to suppose that their lattice parameters are $(3a_{AC} + a_{BC})/4$, $(a_{AC} + a_{BC})/2$ and $(a_{AC} + 3a_{BC})/4$, respectively. Here, a_{AC} and a_{BC} are the lattice parameters of the pure end compounds AC and BC, respectively. The reasons for introducing this assumption on the size of the cube are to avoid more variables and to simplify the model as far as possible. In addition, based on the above assumption, although it is not necessary, the lattice parameters of $A_{1-x}B_xC$ solid solutions can be identified to follow Vegard's law strictly according to the binomial Bernoulli distribution. The atomic positions and distorted features are given in appendix 1; all bond lengths and bond angles in each unit cell can be expressed with only one variable p . A more complicated model is also considered as given in appendix 2.

Keating's model [23], on the strain-energy expression of diamond or zincblende structure with VFF theory, has been widely applied. Martin [24] considered further the effect of point-ion Coulombic forces on the strain energy. Afterwards, the phenomenological VFF theory was simplified by Harrison and the strain energy can be written as [11, 22]:

$$E_s = \frac{1}{2}C_0 \sum_{\text{bond}} \left(\frac{d - d_0}{d_0} \right)^2 + \frac{1}{2}C_1 \sum_{\text{angle}} (\delta\theta)^2. \quad (2)$$

Here, d is the distorted bond length, d_0 is the unstretched bond length in the pure end compounds, and $\delta\theta$ is the deviation from the bond angle of a rectangular tetrahedron. C_0 and C_1 are the radial bond-stretching and angular bond-bending force constants, respectively. They can be obtained with the elastic constants c_{11} and c_{12} and the lattice constant a [11, 12] as follows:

$$\begin{aligned} C_0 &= \frac{3}{16}a^3(c_{11} + 2c_{12}) \\ C_1 &= \frac{1}{32}a^3(c_{11} - c_{12}). \end{aligned} \quad (3)$$

For the cross bond such as A–C–B, we select

$$C_1 = \frac{1}{2}(C_1^{AC} + C_1^{BC}). \quad (4)$$

Equation (2) is used to calculate the strain energies and to determine the equilibrium atomic positions in the five distorted unit cells. The first term in equation (2) extends over all nearest-neighbour atom pairs, standing for two-body interactions. The second term, standing for three-body interactions, extends over all bond angles around every atom. Many-body interactions more than three-body are much smaller and can be neglected as claimed by Keating [23].

The equilibrium bond lengths and the strain energies of the five distorted unit cells can be easily found. Only those bond lengths and bond angles located inside each distorted unit cell need to be counted. The final strain-energy expression depends only on one variable p or δ . Under the assumption that the deviation δ is small, the strain-energy expression is minimized with respect to δ . Finally the equilibrium bond lengths and strain energy at any composition x can be calculated according to

$$\bar{Y}(x) = \frac{\sum_n W(n)P(n, x)Y^{(n)}}{\sum_n W(n)P(n, x)}. \quad (5)$$

Here, $Y^{(n)}$ stands for a bond length or strain energy in such a distorted unit cell with n B-type atoms and $4 - n$ A-type atoms; $W(n)$ is the number of that bond length as shown in table 1. For the strain energy E_s , $W(n)$ is always equal to 1 in each distorted unit cell. $\bar{Y}(x)$ is the averaged value for that bond length or strain energy.

Table 1. Number of bonds in the five distorted unit cells of $A_{1-x}B_xC$ solid solutions ($n = 0, 1, 2, 3, 4$).

| Bond | A–C | B–C | C–A–C | C–B–C | A–C–A | A–C–B | B–C–B |
|--------|------------|------|------------|-------|---------------------|------------|--------------|
| $W(n)$ | $4(4 - n)$ | $4n$ | $6(4 - n)$ | $6n$ | $(n^2 - 7n + 12)/2$ | $n(4 - n)$ | $n(n - 1)/2$ |

3. Results

The FDUC model is applied to 18 $A_{1-x}B_xC$ systems; the bond force constants and lattice parameters listed in [11] are used as the input parameters. As examples, the first- and second-neighbour bond lengths of cation-sharing $GaAs_xP_{1-x}$ and anion-sharing $Ga_{1-x}In_xAs$ are shown in figures 2, 3, 4 and 5, respectively. The experimental values are respectively quoted from [5] and [3] for $GaAs_xP_{1-x}$ and $Ga_{1-x}In_xAs$. The strain energies of four systems are shown in figure 6. It can be seen that all bond lengths are in good agreement with those from EXAFS, with a deviation of about 0.01 Å. Comparing the FDUC model with the FST model [5], we find that the former is better. The FDUC model can give all first- and second-neighbour bond lengths, whereas the FST model can only explain the first-neighbour bond lengths and partial second-neighbour bond lengths. The two models are very similar with the same distributions, and the obtained bond lengths are almost the same. This verifies indirectly that the FST model is also reasonable but not perfect from the energetic point of view.

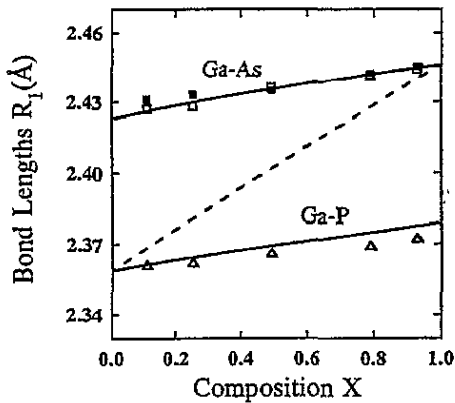


Figure 2. First-nearest-neighbour bond lengths in $\text{GaAs}_x\text{P}_{1-x}$ solid solutions versus composition x . Full curves are values calculated from the model; symbols are experimental values from EXAFS quoted from [5]; and broken line is expected from Vegard's law.

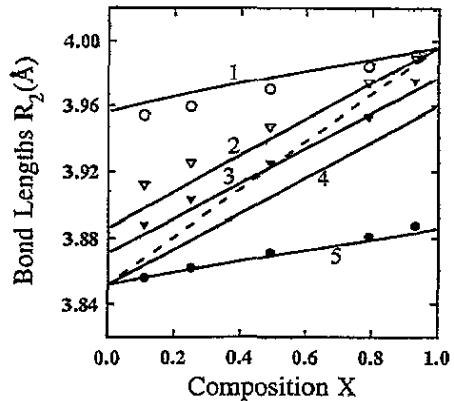


Figure 3. Second-nearest-neighbour bond lengths in $\text{GaAs}_x\text{P}_{1-x}$ solid solutions versus composition x . Full curves 1, 2, 3, 4 and 5 are respectively Ga-As-Ga, As-Ga-As, As-Ga-P, P-Ga-P and Ga-P-Ga bond lengths calculated from the model; symbols are experimental values from EXAFS quoted from [5]; and broken line is expected from Vegard's law.

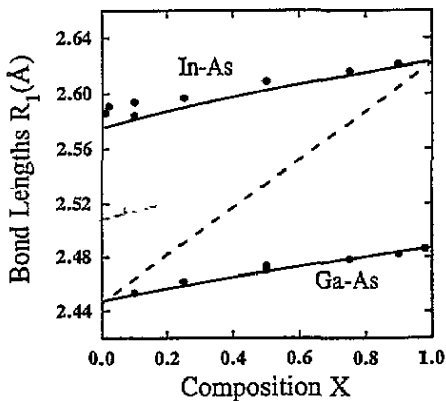


Figure 4. First-nearest-neighbour bond lengths in $\text{Ga}_x\text{In}_{1-x}\text{As}$ solid solutions versus composition x . Full curves are values calculated from the model; symbols are experimental values from EXAFS quoted from [2]; and broken line is expected from Vegard's law.

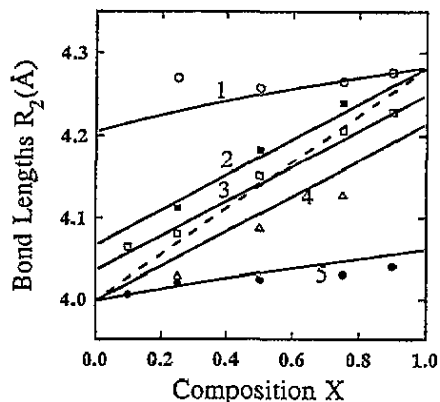


Figure 5. Second-nearest-neighbour bond lengths in $\text{Ga}_{1-x}\text{In}_x\text{As}$ solid solutions versus composition x . Full curves 1, 2, 3, 4 and 5 are respectively As-In-As, In-As-In, In-As-Ga, Ga-As-Ga and As-Ga-As bond lengths calculated from the model; symbols are experimental values from EXAFS quoted from [2]; and broken line is expected from Vegard's law.

Although in zincblende-type $\text{A}_{1-x}\text{B}_x\text{C}$ solid solutions, atoms deviate from the ideal lattice positions and construct five distorted unit cells, by averaging the five distorted unit cells the regular one as implied by VCA can be obtained. Therefore, long-range order is still preserved, as indicated by x-ray diffraction. That is to say, the local structure distortion does not destroy the long-range periodicity.

A more detailed consideration about the FDUC model is given in appendix 2. For the unit cells with $n = 1$ and $n = 3$, there are almost no differences in the results obtained from

appendix 1 and appendix 2. The divergence of angle α from 90° is less than 0.02° and that of the lattice parameter a from a_0 is about 0.002 \AA , which leads to a negligible divergence in the obtained bond lengths. For the unit cell with $n = 2$, a slightly larger divergence is found. Especially for the second-neighbour bond lengths (R_{ACA} , R_{ACB} and R_{BCB}) the largest divergence from the EXAFS results [5] reaches about 0.02 \AA . We also consider the other distorted features in this unit cell with or without the atomic position shift in the middle xy plane; meanwhile, $a = b = c$, $\alpha = \beta = 90^\circ \neq \gamma$, or $a = b \neq c$, $\alpha = \beta = \gamma = 90^\circ$. Comparing these different distorted configurations, we find that the one given in appendix 1 provides the best agreement with EXAFS results. Because the uncertainty of bond lengths obtained from EXAFS is at the level of 0.01 \AA and fewer experimental results are available, especially for the second-neighbour bond lengths, a more accurate distorted configuration is difficult to construct. We believe that the FDUC model is sufficient to describe the local structure distortion in zincblende-type solid solutions.

Using the Keating potential [23], Schabel and Martins (SM) [16] analysed the structural relaxations of pseudobinary III-V and II-IV semiconductor alloys with large periodic supercells. Cai and Thorpe [18], with the Kirkwood potential [21], studied the length-mismatch problem and gave an analytic solution under the assumptions that the force parameters do not vary from site to site and that the unstrained atomic radii are additive. Obviously their first assumption is inappropriate. For this reason, the effective-medium approximation was introduced to solve the problem due to the force parameter disorder. In this paper, by use of Harrison's model [11, 22] to describe the strain energy, we propose a completely different local structural model. The local structures in zincblende-type solid solutions can be described by five distorted unit cells at any composition. The results of SM and CT as well as ours for both the first- and second-neighbour bond lengths are in general agreement. It also demonstrates that the Kirkwood model, the Keating model and the Harrison model, used to describe the strain energy in zincblende-type alloys, are equivalent. Our work gives the microscopic distorted configuration in zincblende-type solid solutions. We believe that the local distorted configuration is helpful to understand the properties of these solid solutions. For a certain coordination environment, the interatomic distances should be relatively fixed. The dependence of bond lengths on composition is the result of averaging the different coordination environments, which corresponds to different bond lengths. Strictly speaking, bond lengths in these alloys do not vary linearly with composition as indicated by SM [16] and CT [18], but the deviations from linearity are small and can almost be neglected.

We also notice the model of Newman *et al* [11], which deals with five order compounds with two or three variables. It was applied to 18 systems and can give the bond lengths at composition $x = 0.25, 0.50$ and 0.75 . The first-neighbour bond lengths are in very good agreement with those from EXAFS, but the second-neighbour bond lengths are not. For comparison, their results about the first-neighbour bond lengths are also listed in table 2.

The calculated strain energy E_s as a function of composition has the shape of a parabola and presents a maximum at about composition $x = 0.5$ as shown in figure 6. It is compared with the excess enthalpy ΔH_m [11, 25] of mixing of an alloy as in the regular solution model, $\Delta H_m = x(1-x)\Omega$. The interaction parameter E is obtained by using the equation $E_s = x(1-x)E$ to fit the strain energy. The calculated E is very close to the experimental Ω (kcal mol^{-1}) as listed in table 2. It seems to imply that zincblende-type solid solutions can be treated as regular solutions, and the excess enthalpy of mixing ΔH_m of the alloys is mainly the contribution of the strain energy. The larger the lattice parameter difference Δa of the two pure end compounds, the greater is the strain energy E_s or the parameter E . Figure 7 shows the variation of the interaction parameter E with the difference of Δa

Table 2. Relative average slopes of bond lengths versus composition x and strain energies of $A_{1-x}B_xC$ solid solutions. Results are compared with those determined from experiments and from the theory of Newman, Shen and Teng (NST). The experimental relative slopes and the interaction parameters Ω in kcal mol⁻¹ as well as NST theory are quoted from [11, 25].

| $A_{1-x}B_xC$ | S_1 | EXAFS | NST | S_2 | S_3 | S_4 | S_5 | E | Ω | NST |
|------------------|-------|-------------------|-----------|-------|-------|-------|-------|-------|--------------|-------|
| $Al_{1-x}Ga_xAs$ | 0.25 | | 0.27,0.28 | 0.25 | 0.76 | 0.76 | 0.75 | 0.001 | 0.0 | 0.001 |
| $Al_{1-x}Ga_xP$ | 0.24 | | 0.27,0.26 | 0.24 | 0.76 | 0.76 | 0.75 | 0.005 | | 0.005 |
| $Al_{1-x}Ga_xSb$ | 0.25 | | 0.25,0.25 | 0.25 | 0.76 | 0.76 | 0.75 | 0.020 | 0.0 | 0.023 |
| $InP_{1-x}As_x$ | 0.24 | | 0.18,0.24 | 0.24 | 0.76 | 0.76 | 0.75 | 0.494 | 0.4 | 0.469 |
| $AlP_{1-x}As_x$ | 0.25 | | 0.25,0.28 | 0.25 | 0.76 | 0.76 | 0.75 | 0.626 | | 0.723 |
| $GaAs_xP_{1-x}$ | 0.24 | 0.18[4],0.24,0.25 | 0.24,0.30 | 0.25 | 0.77 | 0.74 | 0.75 | 0.677 | 0.4,1.0 | 0.806 |
| $Al_{1-x}In_xSb$ | 0.24 | | 0.19,0.26 | 0.24 | 0.76 | 0.76 | 0.75 | 1.409 | 0.6 | 1.433 |
| $Ga_{1-x}In_xSb$ | 0.24 | 0.21,0.22 | 0.20,0.27 | 0.25 | 0.77 | 0.75 | 0.77 | 1.710 | 1.47,1.9 | 1.821 |
| $InAs_{1-x}Sb_x$ | 0.24 | | 0.18,0.25 | 0.24 | 0.76 | 0.76 | 0.75 | 2.066 | 2.25,2.9 | 1.986 |
| $Al_{1-x}In_xAs$ | 0.25 | | 0.20,0.29 | 0.25 | 0.76 | 0.76 | 0.75 | 2.262 | 2.5 | 2.426 |
| $Ga_{1-x}In_xAs$ | 0.24 | 0.23,0.20 | 0.20,0.28 | 0.24 | 0.76 | 0.75 | 0.76 | 2.283 | 1.65,2.0,3.0 | 2.430 |
| $Al_{1-x}In_xP$ | 0.24 | | 0.20,0.26 | 0.24 | 0.76 | 0.76 | 0.75 | 2.625 | | 2.693 |
| $GaAs_{1-x}Sb_x$ | 0.25 | | 0.22,0.31 | 0.25 | 0.76 | 0.76 | 0.75 | 2.776 | 4.0,4.5 | 3.914 |
| $Ga_{1-x}In_xP$ | 0.24 | 0.20,0.24 | 0.20,0.27 | 0.24 | 0.76 | 0.75 | 0.76 | 2.890 | 3.25,3.50 | 3.067 |
| $AlAs_{1-x}Sb_x$ | 0.25 | | 0.21,0.30 | 0.25 | 0.76 | 0.76 | 0.75 | 3.293 | | 3.745 |
| $InP_{1-x}Sb_x$ | 0.24 | | 0.15,0.28 | 0.24 | 0.76 | 0.76 | 0.75 | 4.812 | | 4.578 |
| $GaP_{1-x}Sb_x$ | 0.25 | | 0.19,0.34 | 0.25 | 0.76 | 0.76 | 0.75 | 6.319 | | 7.314 |
| $AlP_{1-x}Sb_x$ | 0.24 | | 0.18,0.31 | 0.24 | 0.76 | 0.76 | 0.75 | 6.717 | | 7.339 |

of lattice parameters of the two pure end compounds. Approximately, we can obtain the relation: $E = 14.6(\Delta a)^2$. Here the units of E and Δa are kcal mol⁻¹ and Å, respectively.

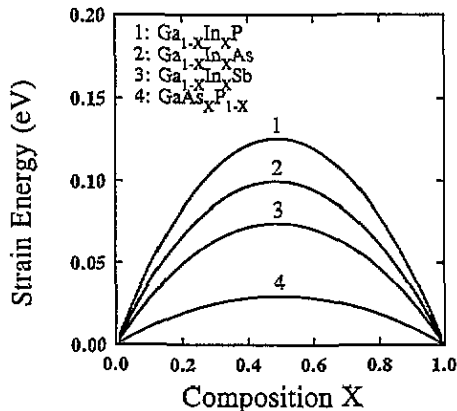


Figure 6. Calculated strain energies of $\text{Ga}_{1-x}\text{In}_x\text{P}$, $\text{Ga}_{1-x}\text{In}_x\text{As}$, $\text{Ga}_{1-x}\text{In}_x\text{Sb}$ and $\text{GaAs}_x\text{P}_{1-x}$ solid solutions in an averaged unit cell.

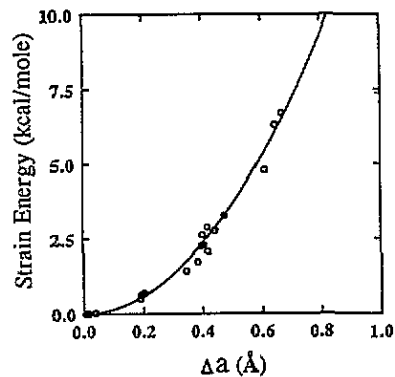


Figure 7. Variation of interaction parameter E (or strain energy E_s) with the difference Δa of lattice parameters of the two pure end compounds. The open circles are values obtained from the FDC model, which follows roughly the relation $E = 14.6(\Delta a)^2$ as indicated by the full curve.

The composition dependence of both the first- and second-neighbour bond lengths is approximately linear. The slope of the variation of near-neighbour bond lengths with composition is a structural characteristic quantity. Because the averaged bond lengths can be described with the VCA model as indicated by x-ray diffraction, for the $\text{A}_{1-x}\text{B}_x\text{C}$ solid solutions, the variation of first-neighbour bond lengths R_{AC} and R_{BC} should have the same slope S_1 while the slope of the second-neighbour bond lengths R_{CAC} and R_{CBC} is S_2 . For the bond lengths R_{BCB} , R_{ACA} and R_{ACB} , their variation with composition have slopes S_3 , S_4 and S_5 , respectively, where $S_3 + S_4 = 2S_5$. If we define S_1^V and S_2^V as the slopes expected from Vegard's law for the variation of first- and second-neighbour bond lengths, respectively, then the relative slopes of near-neighbour bond lengths are convenient for comparison in different zincblende-type solid solutions. Table 2 lists all relative slopes obtained from experiments and from this model. It demonstrates that S_1/S_1^V and S_2/S_2^V are almost the same and about 0.24–0.25, whereas S_3/S_2^V , S_4/S_2^V and S_5/S_2^V are also the same and about 0.75–0.76. Slopes S_1 calculated from this model are in agreement with experimental values. According to the results above, both the first- and second-neighbour bond lengths in $\text{A}_{1-x}\text{B}_x\text{C}$ solid solutions can be roughly (not accurately) expressed as:

$$\begin{aligned}
 R_{AC} &= \left(\sqrt{3}/16\right) [4a_{AC} + (a_{BC} - a_{AC})x] \\
 R_{BC} &= \left(\sqrt{3}/16\right) [3a_{BC} + a_{AC} + (a_{BC} - a_{AC})x] \\
 R_{CAC} &= \left(\sqrt{2}/8\right) [4a_{AC} + (a_{BC} - a_{AC})x] \\
 R_{CBC} &= \left(\sqrt{2}/8\right) [3a_{BC} + a_{AC} + (a_{BC} - a_{AC})x] \\
 R_{ACA} &= \left(\sqrt{2}/8\right) [4a_{AC} + 3(a_{BC} - a_{AC})x] \\
 R_{ACB} &= \left(\sqrt{2}/16\right) [a_{BC} + 7a_{AC} + 6(a_{BC} - a_{AC})x] \\
 R_{BCB} &= \left(\sqrt{2}/8\right) [a_{BC} + 3a_{AC} + 3(a_{BC} - a_{AC})x].
 \end{aligned} \tag{6}$$

Here, a_{AC} and a_{BC} are the lattice parameters of the pure end compounds AC and BC, respectively. Equation (6) does not depend on any variable. Both the first- and second-neighbour bond lengths can be easily found through the lattice parameters.

The local distortions around a B impurity doped in the AC host crystal correspond to the case of the distorted unit cell with $n = 1$, as indicated in appendix 1. With the inclusion of a B atom the lattice parameter is expanded (or compressed). Meanwhile, the first and second neighbours around a B impurity are pushed aside (or pulled in), while the third or more distant neighbours stay in their regular positions with no shift. This is because the distortions decrease rapidly as distance increases. Similarly, the local distortions around an A impurity doped in the BC host crystal correspond to the case of the distorted unit cell with $n = 3$.

The FDUC model requires only knowledge of the lattice parameters and the bond force constants (or bulk moduli) of the pure end compounds. It can predict both the first- and second-neighbour equilibrium bond lengths and strain energy at any composition in zincblende-type solid solutions. The results obtained agree very well with those from experiments. The success of the FDUC model in getting reasonable bond lengths suggests that long-range interactions are, indeed, unimportant, and that the assumption on the size of the cube for the five distorted unit cells is feasible. EXAFS experiments [5] indicate that the anion C sublattice is more stable, which tends to maintain the same structure as in the pure end compounds, while the mixed cation sublattice composed of displaceable atoms is more flexible, which approaches the VCA model in $A_{1-x}B_xC$ solid solutions. In the FDUC model, these distorted features are involved in the five distorted unit cells. A more detailed structure model can perhaps obtain more accurate results, but the improvement will be much smaller. Summarizing the results, it can be concluded that FDUC model is reasonable and effective in describing the local structures of zincblende-type solid solutions.

4. Conclusion

In this paper we investigate the local atomic structures of zincblende-type solid solutions and propose a FDUC model. This model predicts the local distorted feature in zincblende-type random solid solutions. Under the VFF approximation, the obtained first- and second-neighbour bond lengths agree well with EXAFS results. Further, we give a simple expression for both the first- and second-neighbour bond lengths, which can be obtained

from information only about lattice parameters. The calculated values of the strain energy demonstrate that the local elastic distortions are the primary physical factor deciding the excess enthalpy of mixing ΔH_m .

Acknowledgments

This research was supported by the Chinese National Science Foundation and a grant from the State Science and Technology Commission of China (for key research project in Climbing Programme).

Appendix 1

Here we summarize the information required to find the strain energies and bond lengths of the five distorted unit cells shown in figure 1. First, the five distorted unit cells retain cubic shape and their lattice parameters are respectively fixed to those values evaluated from Vegard's law. The origin in each unit cell is chosen at the lower left corner. The two unit cells with $n = 0$ and $n = 4$ are completely the same as in the pure end compounds AC and BC, respectively. There are no distortions and shifts of atomic positions in them.

For the unit cells with $n = 1$, the atomic positions of ten C atoms, one B and three A atoms are as follows:

$$\begin{array}{ll}
 \text{C1} : [0, 0, 0] & \text{C2} : [0, p/2, p/2] \\
 \text{C3} : [p/2, 0, p/2] & \text{C4} : [p/2, p/2, 0] \\
 \text{C5} : [a/2, a/2, a] & \text{C6} : [a, a/2, a/2] \\
 \text{C7} : [a/2, a, a/2] & \text{C8} : [0, a, a] \\
 \text{C9} : [a, 0, a] & \text{C10} : [a, a, 0] \\
 \text{B1} : [p/4, p/4, p/4] & \text{A1} : [a/4, (5a + p)/8, (5a + p)/8] \\
 \text{A2} : [(5a + p)/8, a/4, (5a + p)/8] & \text{A3} : [(5a + p)/8, (5a + p)/8, a/4].
 \end{array} \tag{A1.1}$$

The unit cell with $n = 3$ has completely the same distorted features as in that with $n = 1$; its atomic positions can also be written as in equation (A1.1) if we alter the B atom for one A atom, and the three A atoms for the three B atoms.

Let us look at the unit cell with one B atom and three A atoms. Its lattice parameter expands (or compresses) from a_{AC} to $(a_{BC} + 3a_{AC})/4$. The nearest three C neighbours of a B atom are pushed aside (or pulled in). These distortions propagate to the three next-nearest-neighbour A atoms, and stop at the third-neighbour C atoms, which are still situated at the regular face centres. The four A and B atoms, due to the actions of four C neighbours, are forced to locate at the centroid of such a tetrahedron consisting of four C atoms, respectively.

The atomic positions of ten C atoms, two B and two A atoms in the unit cell with $n = 2$ are located at:

$$\begin{aligned}
C1 : [0, 0, 0] & & C2 : [0, p/2, p/2] \\
C3 : [p/2, 0, p/2] & & C4 : [a/2, a/2, 0] \\
C5 : [a/2, a/2, a] & & C6 : [a, (2a - p)/2, p/2] \\
C7 : [(2a - p)/2, a, p/2] & & C8 : [0, a, a] \\
C9 : [a, 0, a] & & C10 : [a, a, 0] \\
B1 : [(a + p)/8, (a + p)/8, p/4] & & B2 : [(7a - p)/8, (7a - p)/8, p/4] \\
A1 : [(5a + p)/8, (3a - p)/8, (2a + p)/4] & & \\
A2 : [(3a - p)/8, (5a + p)/8, (2a + p)/4]. & &
\end{aligned} \tag{A1.2}$$

In this unit cell, there are two A atoms and two B atoms. Its lattice parameter is $(a_{AC} + a_{BC})/2$ according to Vegard's law. The four C atoms, in the middle xy plane of the unit cell, shift along the z direction and have an equal shift along the x direction or y direction. The four A and B atoms also locate respectively at the centroid of such a tetrahedron consisting of four C atoms. If the atomic positions of the two B atoms exchange with those of the two A atoms, as we expect, the distorted features of the unit cell remain invariable.

Here, we assume that the five distorted unit cells are still cubic, which greatly simplifies the local structure model and reduces the number of variables. In each distorted unit cell, the bond lengths, bond angles and strain energy depend only on the variable p or δ , defined as

$$p = a(1 + \delta). \tag{A1.3}$$

Here, δ is a small quantity, and p is very close to the lattice parameter evaluated from Vegard's law. Under the condition that the strain energy is minimized, all equilibrium bond lengths, bond angles and strain energy are obtained.

Appendix 2

For the five distorted unit cells, more complicated distorted features are considered. Here the assumption on the size of the cube is removed. We define \hat{a} , \hat{b} and \hat{c} as the axial vectors, and α , β , γ are the relative angles. For the distorted unit cells with $n = 1$ and $n = 3$, a reasonable assumption is that $a = b = c$, and $\alpha = \beta = \gamma$. We define

$$a = a_0(1 + \delta_1) \quad p = a_0(1 + \delta_2) \quad \alpha = 90^\circ + \delta_3. \tag{A2.1}$$

Here a_0 is the lattice parameter expected from Vegard's law. The atomic positions in the two unit cells are easily obtained from those in appendix 1 by the following transformation matrix:

$$\mathbf{T} = \begin{pmatrix} 1 & \cos \alpha & \cos \alpha \\ 0 & \sin \alpha & \sin \alpha \cos \theta \\ 0 & 0 & \sin \alpha \sin \theta \end{pmatrix}. \tag{A2.2}$$

Namely, $\mathbf{X}_2 = \mathbf{T}\mathbf{X}_1$, where \mathbf{X}_1 and \mathbf{X}_2 represent the atomic positions in the unit cell with $n = 1$ or $n = 3$ in appendix 1 and 2, respectively. Also, $\cos \theta = \cos \alpha / (1 + \cos \alpha)$. In the

two unit cells, the distance a need not equal the lattice parameter a_0 and the angle is not fixed to be 90° . We introduce three variables δ_1 , δ_2 and δ_3 to describe the distorted features; δ_1 , δ_2 and δ_3 are small quantities and can be determined by minimizing the distorted energy.

For the distorted unit cell with $n = 2$, we assume that $a = b \neq c$ and $\alpha = \beta = 90^\circ$, $\gamma \neq 90^\circ$. Four variables are introduced to describe the distorted features,

$$\begin{aligned} a &= a_0(1 + \delta_1) & c &= a_0(1 + \delta_2) \\ p &= a_0(1 + \delta_3) & \gamma &= 90^\circ + \delta_4. \end{aligned} \quad (\text{A2.3})$$

The atomic positions in the unit cell can also be obtained from those in appendix 1 by the transformation matrix

$$\mathbf{T} = \begin{pmatrix} 1 & \cos \alpha & 0 \\ 0 & \sin \alpha & 0 \\ 0 & 0 & c/a \end{pmatrix}. \quad (\text{A2.4})$$

Similarly, the equilibrium atomic positions, bond lengths and strain energy can also be obtained by minimizing the distorted energy.

References

- [1] Mikkelsen J C Jr and Boyce J B 1982 *Phys. Rev. Lett.* **49** 1412
- [2] Mikkelsen J C Jr and Boyce J B 1983 *Phys. Rev. B* **28** 7130
- [3] Balzarotti A, Motta N, Kisiel A, Zimnal-Starnawska M, Czyzyk M T and Podgórný M 1985 *Phys. Rev. B* **31** 7526
- [4] Pong W F, Mayanovic R A, Bunker B A, Furdyna J K and Debska U 1990 *Phys. Rev. B* **41** 8440
- [5] Wu Z, Lu K, Wang Y, Dong J, Li H, Li C and Fang Z 1993 *Phys. Rev. B* **48** 8694
- [6] Pong W F, Mayanovic R A and Bunker B A 1989 *Physica B* **158** 617
- [7] Sher A, van Schilfgaard M, Chen A-B and Chen W 1987 *Phys. Rev. B* **36** 4279
- [8] Tsai M-H, Dow J D, Newman K E and Kasowski R V 1990 *Phys. Rev. B* **41** 7744
- [9] Chen A B and Sher A 1985 *Phys. Rev. B* **32** 3695
- [10] Balzarotti A 1987 *Physica B* **146** 150
- [11] Newman K E, Shen J and Teng D 1989 *Superlat. Microstruct.* **6** 245
- [12] Martins J L and Zunger A 1984 *Phys. Rev. B* **30** 6217
- [13] Srivastava G P, Martins J L and Zunger A 1985 *Phys. Rev. B* **31** 2561
- [14] Mbaye A A, Wood D M and Zunger A 1988 *Phys. Rev. B* **37** 3008
- [15] Shih C K, Spicer W E, Harrison W A and Sher A 1985 *Phys. Rev. B* **31** 1139
- [16] Schabel M C and Martins J L 1992 *Phys. Rev. B* **43** 11873
- [17] Cai Y and Thorpe M F 1992 *Phys. Rev. B* **46** 15872
- [18] Cai Y and Thorpe M F 1992 *Phys. Rev. B* **46** 15879
- [19] Mousseau N and Thorpe M F 1992 *Phys. Rev. B* **46** 15887
- [20] Podgórný M, Czyzyk M T, Balzarotti A, Letardi P, Motta N, Kisiel A and Zimnal-Starnawska M 1985 *Solid State Commun.* **55** 413
- [21] Kirkwood J G 1939 *J. Chem. Phys.* **7** 506
- [22] Harrison W A 1980 *Electronic Structure and the Properties of Solids* (San Francisco: Freeman)
- [23] Keating P N 1966 *Phys. Rev.* **145** 637
- [24] Martin R M 1970 *Phys. Rev. B* **1** 4005
- [25] Stringfellow G B 1974 *J. Cryst. Growth* **27** 21